

Enhancing Target-unspecific Tasks through a Features Matrix

Fangming Cui¹ Yonggang Zhang² Xuan Wang³ Xinmei Tian⁴ Jun Yu⁵

Abstract

Recent developments in prompt learning of large vision-language models have significantly improved performance in target-specific tasks. However, these prompt optimizing methods often struggle to tackle the target-unspecific or generalizable tasks effectively. It may be attributed to the fact that overfitting training causes the model to forget its general knowledge having strong promotion on target-unspecific tasks. To alleviate this issue, we propose a novel Features Matrix (FM) regularization approach designed to enhance these models on target-unspecific tasks. Our method extracts and leverages general knowledge, shaping a Features Matrix (FM). Specifically, the FM captures the semantics of diverse inputs from a deep and fine perspective, preserving essential general knowledge, which mitigates the risk of overfitting. Representative evaluations demonstrate that: 1) the FM is compatible with existing frameworks as a generic and flexible module, and 2) the FM significantly showcases its effectiveness in enhancing target-unspecific tasks, achieving state-of-the-art performance.

1. Introduction

Large vision-language models such as CLIP (Radford et al., 2021) have attracted increasing attention for remarkable generalization performance. Vision-language models (VLMs) are trained to align textual and visual modalities by leveraging extensive datasets. For instance, a prominent example of such models is CLIP, which has achieved remarkable success across a wide range of downstream tasks (Greer et al., 2024; Sanghi et al., 2021; Etchegaray et al., 2024). CLIP utilizes a large collection of 400 million text-image

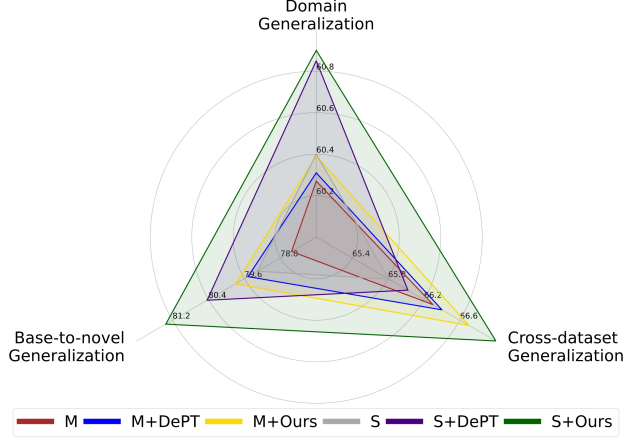


Figure 1. Our method is orthogonal to representative architectures, such as MaPLE (M) and PromptSRC (S), surpassing the existing state-of-the-art easy-to-use DePT by a significant margin.

pairs. One of CLIP’s most appealing features is its ability to perform zero-shot inference. During inference, CLIP utilizes hand-crafted text inputs, known as prompts, to generate classification weights to predict image features, all without requiring any target-specific parameters training.

In contrast to hand-crafted prompts, a model-parameter tuning method has been proposed as prompt learning to automatically learn prompt embeddings (Zhou et al., 2022a). For instance, CoOp (Zhou et al., 2022b) represents the first method that specifically focuses on learning the text embeddings of prompts with few-shot samples training while keeping the CLIP model frozen. Although CoOp (Zhou et al., 2022b) has shown significant performance improvements over hand-crafted prompts in target-specific base classes, it may yield inferior performance compared to the hand-crafted prompt CLIP in generalization tasks, e.g., the novel class of generalization from base-to-novel (see Table 1).

To overcome this challenge, some effective methods (Lu et al., 2022; Zhou et al., 2022a;b; Yao et al., 2023a; Chen et al., 2022) with tuning textual embeddings have been proposed. These methods aim to enhance the performance of novel classes, surpassing the novel performance of the previous CoOp. Although the novel ability of these methods surpasses that of CoOp (67.96%), it is unfortunate that the

¹Shanghai Jiao Tong University ²Hong Kong Baptist University
³Meituan Inc. ⁴University of Science and Technology of China
⁵Harbin Institute of Technology (Shenzhen). Correspondence to: Jun Yu <yujun@hit.edu.cn>.

Table 1. Our method is an easy-to-use design, integrated into CoOp, obtaining a higher average performance (11 datasets) on novel (target-unspecific) classes.

Method	Design	Base	Novel
CLIP (ICML2021)	Hand	69.34	74.22
CoCoOp (CVPR2022)	Tune	80.47	71.69
PLOT (ICLR2023)	Tune	81.24	72.98
CoOp (IJCV2022)	Tune	82.38	67.96
+ DePT (CVPR2024)	Tune	83.66	71.82
+ Kg (CVPR2023)	Tune + Hand	80.73	72.70
+ Ours	Tune + Hand	81.15	74.66

novel ability of these methods still falls short compared to the hand-crafted prompt method (CLIP: 74.22%), as shown in Table 1 (Novel). A possible reason (Zhou et al., 2022a) may be that these prompting methods with tuning text embeddings tend to overfit the downstream data distributions. This overfitting can result in the model losing its inherent generalization capabilities (Yao et al., 2023a) obtained from hand-crafted prompts (Radford et al., 2021).

To alleviate this problem, we propose a novel Features Matrix (FM) with CLIP for target-unspecific tasks. Our method incorporates multiple hand-crafted prompts to extract general information as a pre-trained matrix from frozen CLIP to enhance generalization. The matrix of pre-trained features can delve into the semantics of different hand-crafted prompts finely and deeply, which reduces the risk of forgetting the essential general knowledge of pre-trained CLIP. Importantly, our method is compatible with current prompt learning frameworks for textual or multi-modal prompt learning and serves as a flexible and generic module. As demonstrated in Figure 1, our method integrated to the representative Maple (Khattak et al., 2023a) and PromptSRC (Khattak et al., 2023b), exhibits competitive results in base-to-novel generalization, domain generalization, and cross-dataset generalization across 11 datasets. Meanwhile, our method surpasses the existing state-of-the-art easy-to-use DePT (Zhang et al., 2024) by a significant margin. Our contributions can be summarized as follows:

- The proposed method incorporates multiple hand-crafted prompts with classes to extract general knowledge as a pre-trained features matrix (FM).
- We propose an easy-to-use design, which is compatible with representative textual or multi-modal prompt learning frameworks for adapting CLIP.
- Various target-unspecific tasks (base-to-novel generalization, cross-dataset generalization, and domain generalization) across 11 datasets demonstrate that our method showcases its effectiveness.

2. Preliminaries

Notations. Considering a pre-trained VLM, let $\mathcal{E}_v(\cdot)$ be its image encoder and $\mathcal{E}_t(\cdot)$ be its text encoder. The image encoder transforms input images into feature embeddings, capturing the visual information within the images. The text encoder generates representations for word embedding sequences, capturing the semantic information conveyed by the text prompts \mathbf{p} . Generally, a hand-crafted prompt \mathbf{p} may have the form of “a photo of a [Class]”. In this paper, \mathbf{x} represents an arbitrary image, and l denotes the label.

Hand-Crafted CLIP. During the pre-training phase of CLIP (Radford et al., 2021), the image and text encoders are jointly trained on large-scale text-image pairs using a contrastive loss. This loss maximizes the cosine similarity between matching pairs and minimizes it between non-matching pairs, enabling the encoders to learn aligned visual and textual representations effectively. The final prediction score between the image \mathbf{x} and text prompt \mathbf{p} is computed using contrastive learning. The final prediction probability of alignment is computed by the matching score as follows:

$$p(l = k | \mathbf{x}) = \frac{\exp \{ \cos(\mathcal{E}_t(\mathbf{p}_k), \mathcal{E}_v(\mathbf{x})) / \tau \}}{\sum_{k'=1}^K \exp \{ \cos(\mathcal{E}_t(\mathbf{p}_{k'}), \mathcal{E}_v(\mathbf{x})) / \tau \}}, \quad (1)$$

where l is the label of \mathbf{x} , $\cos(\cdot, \cdot)$ stands for cosine similarity between two vectors, and $\tau > 0$ represents a temperature parameter. Here, the classifier consists of K textual features derived from prompts $\{\mathbf{p}_{k'}\}_{k'=1}^K$, where the prompt $\mathbf{p}_{k'}$ for the k' -th class may have the form of “a photo of a”.

Textual Prompting. In textual prompting, the class name is retained as prior knowledge, while the word embeddings (referred to as context) of prompts are treated as learnable parameters, as shown in CoOp (Zhou et al., 2022b) and Co-CoOp (Zhou et al., 2022a) of Figure 2. By modeling these context embeddings as trainable parameters, the model can optimize the prompts based on the specific requirements, enhancing the alignment between images and prompts. For class k , the tuning feature of the text encoder is denoted as t_k^{tun} in a dataset with total K classes. The final prediction probability of cross-entropy loss for two-modalities alignment is computed as:

$$p(l = k | \mathbf{x}) = \frac{\exp \{ \cos(t_k^{tun}, \mathcal{E}_v(\mathbf{x})) / \tau \}}{\sum_{k'=1}^K \exp \{ \cos(t_{k'}^{tun}, \mathcal{E}_v(\mathbf{x})) / \tau \}}, \quad (2)$$

where $\cos(\cdot, \cdot)$ stands for cosine similarity, and τ represents a temperature parameter. In some learned text embedding methods, the method aligns with the CoOp methodology by setting the embeddings to be shared across different classes. During the inference phase, the prompts, along with the learned embeddings, can generate textual features that are used for classification purposes. By leveraging

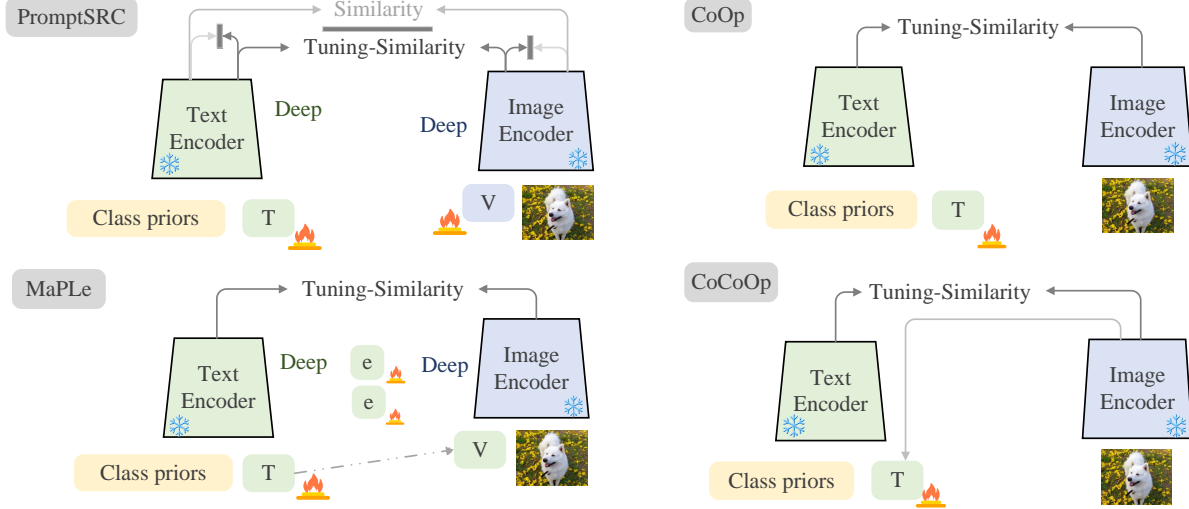


Figure 2. Illustration of representative textual prompting frameworks (CoOp and CoCoOp) and multi-modal prompting frameworks (MaPLE and PromptSRC). We propose a flexible and generic design, which is compatible with these representative architectures. In the figure, "snowflake pattern" represents parameter freezing, "flame pattern" represents learnable pattern, "Deep" represents learnable tokens embedded in several layers of the encoder, where "T" represents learnable text embedding, "V" represents learnable visual embedding, "Class priors" represents which category it belongs to, "Tuning Similarity" represents the calculation of cosine similarity for fine-tuning architecture, and the light gray "Similarity" represents the calculation of cosine similarity for frozen architecture. In the MaPLE architecture diagram, the "e" represents the matrix function that connects the encoders of two modalities in several layers.

these learned embeddings, the model can produce more effective representations, leading to improved target-specific classification performance (Zhou et al., 2022b).

Multi-Modal Prompting. Based on textual deep prompting, this design uses only a limited number of trainable parameters in the image encoder, as shown in MaPLE (Khattak et al., 2023a) and PromptSRC (Khattak et al., 2023b) of Figure 2. The visual prompts are introduced at every transformer layer's input space. In the visual branch, the input image $\mathbf{x} \in \mathbb{R}^{C \times H \times W}$ is divided into M patches. And, a tuning embedding of class i_{class} is appended with the input patches. The foundation of vision prompting is ViT (Vision Transformer) (Dosovitskiy et al., 2020) backbone, which shares the same image encoder as CLIP. Let \mathcal{P}_v denote the visual embeddings of prompts, and the image encoder processes the input tokens to generate tuning visual features, as follows (Jia et al., 2022):

$$\tilde{\mathbf{x}}_p = \{\mathcal{P}_v, i_{class}, i_1, i_2, \dots, i_M\}, \quad (3)$$

the tuning visual embeddings are introduced in the image encoder for deep prompt tuning.

3. Methodology

3.1. Challenge and Motivation

As shown in Table 1, such as textual prompt (Zhou et al., 2022a;b; Yao et al., 2023a; Lu et al., 2022) and multi-modal

prompting (Chen et al., 2022), have shown significant improvements in target-specific base classes. However, these methods often suffer from overfitting, leading to poor generalization in novel classes. To improve the novel performance of models, prompting regularization involves constraining the pre-trained and fine-tuning features in the text branch through computed loss. This constraint helps prevent forgetting general knowledge and ensures that the model retains essential information for downstream tasks. The objective of this design is to activate and maintain the pre-trained general knowledge, leveraging its remarkable generalization abilities to mitigate performance degradation when dealing with target-unspecific classes.

Recently, KgCoOp (Yao et al., 2023a) incorporates the constraint with $L1$ loss on fine-tuning feature with the pre-trained feature for the textual branch, avoiding the loss of CLIP's original generalization capability. However, the novel performance of KgCoOp (72.70%) is still lower than CLIP (74.22%), as shown in Table 1 (Novel). It may be attributed to the fact that this single hand-crafted prompting regularization with CLIP cannot fully release and excavate the diversity semantics for utilizing essential general knowledge (Khattak et al., 2023b).

3.2. Proposed Features Matrix (FM)

To tackle this challenge and problem, we propose a novel design called Features Matrix (FM) for enhancing target-

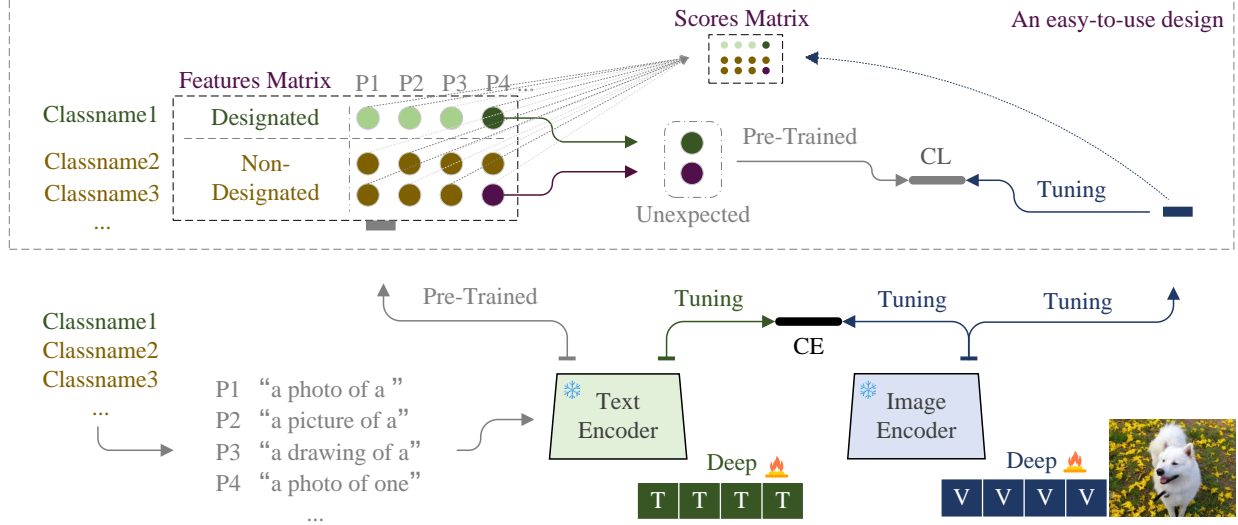


Figure 3. Illustration of our easy-to-use method. We propose a novel Features Matrix (FM) for enhancing target-unspecific tasks. Our method incorporates multiple hand-crafted prompts with classes to extract general knowledge as a pre-trained features matrix. Various generalization tasks across 11 datasets demonstrate that our method outperforms existing prompt learning methods.

unspecific tasks. Our method incorporates multiple hand-crafted prompts with classes of the same datasets to extract general information as a pre-trained features matrix from CLIP to enhance generalization. In this way, we can explore and excavate the semantic information brought by each hand-crafted prompt more finely and deeply. By specifically aligning these multiple pre-trained hand-crafted unexpected features and tuning image features, our method aims to enhance the model’s generalization and robustness. This involves focusing on indistinguishable features that pose a challenge to the model during training.

As shown in Figure 3, we employ a set of hand-crafted prompt templates (P1, P2, P3, P4, etc) as inputs in the text encoder of pre-trained frozen CLIP. These prompt templates such as “a photo of one”, “a photo of a”, “a picture of a”, “a drawing of a”, etc. These prompt templates are from the Prompt Engineering (Radford et al., 2021). In a dataset containing K classes, the input to the text encoder is the frozen embeddings of hand-crafted prompts, consisting of different classes. The output of the frozen text encoder can be viewed as a features matrix, as depicted in Figure 3.

Specifically, we let t denote the sets of pre-trained text features extracted by a frozen text encoder through a set of hand-crafted prompts templates (P1, P2, P3, P4, etc) with classes. In a dataset with total K classes, features belonging to the current label k of image samples are referred to as designated features t_k , while features from other classes are considered non-designated features $t_{\hat{k}}$. Our method computes the matching scores with the cosine distance for each visual output feature v^{tun} and designated pre-trained text

features of the features matrix as $\cos(t_k, v^{tun})$. Similarly, we compute the matching scores between each visual output feature and the non-designated pre-trained text features, denoted as $\cos(t_{\hat{k}}, v^{tun})$. In correspondence with the features matrix, these matching scores can be viewed as a scores matrix, as depicted in Figure 3. Subsequently, we identify the textual features with lower scores (low- β) among the designated features, which is referred to as unexpected designated features set F_{un}^k . Similarly, we identify textual features with higher scores (top- β) among the non-designated features, which are referred to as unexpected non-designated feature sets $F_{un}^{\hat{k}}$. Accordingly, the contrastive loss \mathcal{L}_{CL} of unexpected features similarity is denoted as follows,

$$\mathcal{L}_{CL} = -\log \frac{\exp \{\cos(t_k, v^{tun})\}}{\exp \{\cos(t_k, v^{tun})\} + \exp \{\cos(t_{\hat{k}}, v^{tun})\}}, \quad (4)$$

where $t_k \in F_{un}^k$ and $t_{\hat{k}} \in F_{un}^{\hat{k}}$ as the selected unexpected features for designated unexpected features and non-designated unexpected features. The objective is to explore and excavate the unexpected features of general information. We train the objective for aligning the unexpected text features and tuning visual features, and the contrastive loss \mathcal{L}_{CL} optimizes visual embeddings. For two-modal alignment, let $\mathcal{L}_{CE}(\cdot, \cdot)$ denote the cross-entropy loss with prompts \mathbf{p} for samples \mathcal{S} , as follows,

$$\mathcal{L}_{CE} = \arg \min_{\mathbf{p}} \mathbb{E}_{(\mathbf{x}, y) \sim \mathcal{S}} \mathcal{L} \{ \cos(t^{tun}, v^{tun}), l \}. \quad (5)$$

Accordingly, the objective \mathcal{L}_{total} with a hyper-parameter γ of our method can be formulated as follows,

$$\mathcal{L}_{total} = \mathcal{L}_{CE} + \gamma \mathcal{L}_{CL}. \quad (6)$$

Table 2. Base-to-novel generalization. Our method achieves consistent average performance improvement over different baselines.

(a) Average over 11 datasets				(b) ImageNet				(c) Caltech101				(d) OxfordPets			
Base	Novel	HM		Base	Novel	HM		Base	Novel	HM		Base	Novel	HM	
CoOp	82.69	63.22	71.66	CoOp	76.47	67.88	71.92	CoOp	98.00	89.81	93.73	CoOp	93.67	95.29	94.47
+ Ours	81.15	74.66	77.79	+ Ours	75.85	71.33	73.53	+ Ours	97.58	96.60	97.13	+ Ours	93.78	97.80	95.78
Co	80.47	71.69	75.83	Co	75.98	70.43	73.10	Co	97.96	93.81	95.84	Co	95.20	97.69	96.43
+ Ours	81.68	75.55	78.52	+ Ours	77.35	72.36	74.79	+ Ours	98.61	96.75	97.70	+ Ours	95.33	98.15	96.76
M	82.28	75.14	78.55	M	76.66	70.54	73.47	M	97.74	94.36	96.02	M	95.43	97.76	96.58
+ Ours	84.45	76.53	80.32	+ Ours	78.18	71.38	74.62	+ Ours	98.35	96.11	97.22	+ Ours	95.85	98.22	97.04
S	84.26	76.10	79.97	S	77.60	70.73	74.01	S	98.10	94.03	96.02	S	95.33	97.30	96.30
+ DePT	85.19	76.17	80.43	+ DePT	78.20	70.27	74.02	+ DePT	98.57	94.10	96.28	+ DePT	95.43	97.33	96.37
+ Ours	85.70	77.35	81.32	+ Ours	78.90	71.58	75.07	+ Ours	98.62	95.88	97.27	+ Ours	95.95	97.92	96.95
(e) EuroSAT				(f) UCF101				(g) StanfordCars				(h) Flowers102			
Base	Novel	HM		Base	Novel	HM		Base	Novel	HM		Base	Novel	HM	
CoOp	92.19	54.74	68.69	CoOp	84.69	56.05	67.46	CoOp	78.12	60.40	68.13	CoOp	97.60	59.67	74.06
+ Ours	88.35	65.33	75.13	+ Ours	83.10	78.85	80.94	+ Ours	74.32	76.87	75.58	+ Ours	96.22	72.32	82.57
Co	87.49	60.04	71.21	Co	82.33	73.45	77.64	Co	70.49	73.59	72.01	Co	94.87	71.75	81.71
+ Ours	88.15	70.11	78.12	+ Ours	82.95	77.21	80.00	+ Ours	72.88	76.10	74.46	+ Ours	95.61	74.93	84.03
M	94.07	73.23	82.35	M	83.00	78.66	80.77	M	72.94	74.00	73.47	M	95.92	72.46	82.56
+ Ours	94.22	75.65	83.93	+ Ours	87.33	79.10	83.02	+ Ours	78.66	75.13	76.86	+ Ours	98.21	75.00	85.07
S	92.90	73.90	82.32	S	87.10	78.80	82.74	S	78.27	74.97	76.58	S	98.07	76.50	85.95
+ DePT	92.23	77.90	84.88	+ DePT	87.73	77.70	82.46	+ DePT	80.80	75.00	77.79	+ DePT	98.40	77.10	86.46
+ Ours	95.50	76.85	85.17	+ Ours	88.80	79.50	83.93	+ Ours	80.91	76.51	78.68	+ Ours	98.81	78.10	87.26
(i) Food101				(j) FGVC Aircraft				(k) SUN397				(l) DTD			
Base	Novel	HM		Base	Novel	HM		Base	Novel	HM		Base	Novel	HM	
CoOp	88.33	82.26	85.19	CoOp	40.44	22.30	28.75	CoOp	80.60	65.89	72.51	CoOp	79.44	41.18	54.24
+ Ours	89.98	92.85	91.41	+ Ours	37.32	34.61	35.92	+ Ours	79.12	78.38	78.77	+ Ours	77.10	56.38	65.15
Co	90.70	91.29	90.99	Co	33.41	23.71	27.74	Co	79.74	76.86	78.27	Co	77.01	56.00	64.85
+ Ours	90.61	91.93	91.28	+ Ours	37.87	34.91	36.33	+ Ours	80.32	79.00	79.68	+ Ours	78.90	59.61	67.93
M	90.71	92.05	91.38	M	37.44	35.61	36.50	M	80.82	78.70	79.75	M	80.36	59.18	68.16
+ Ours	90.31	92.81	91.57	+ Ours	42.46	37.62	39.89	+ Ours	82.35	79.81	81.07	+ Ours	83.01	60.98	70.32
S	90.67	91.53	91.10	S	42.73	37.87	40.15	S	82.67	78.47	80.52	S	83.37	62.97	71.75
+ DePT	90.87	91.57	91.22	+ DePT	45.70	36.73	40.73	+ DePT	83.27	78.97	81.06	+ DePT	84.80	61.20	71.09
+ Ours	90.61	92.30	91.45	+ Ours	45.81	39.11	42.20	+ Ours	83.90	80.51	82.20	+ Ours	84.90	62.58	72.07

Consequently, optimizing models with \mathcal{L}_{CL} between the pre-trained textual unexpected features and image tuning features. The \mathcal{L}_{CE} represents two modalities of alignment of deep vision-language prompting. Importantly, our method is compatible with representative prompt learning frameworks as a generic and flexible module for textual prompt learning, such as CoOp and CoCoOp, or multi-modal prompt learning such as MaPLe and PromptSRC.

4. Main Generalization Tasks

4.1. Benchmark Setting

Compared Methods. In three generalization experiments, we compare our method with CLIP (ICML2021) (Radford et al., 2021), CoOp (IJCV2022) (Zhou et al., 2022b),

CoCoOp (CVPR2022) (Zhou et al., 2022a), MaPLe (M) (CVPR2023) (Khatakt et al., 2023a), PromptSRC (S) (ICCV2023) (Khatakt et al., 2023b), FAP (NIPS2024) (Zhou et al., 2024) and existing DePT (CVPR2024) (Zhang et al., 2024). The DePT is an easy-to-use method. We process frozen CLIP using a linear probe method. Comparison methods are based on ViT-B/16 architecture for fair comparison.

Implementation Details. We employ a CLIP model based on the ViT-B/16 architecture. For the PromptSRC-based and MaPLe-based frameworks, we set the visual and textual embedding length to 4. We set the easy-to-use module γ to 0.1 and matching scores (top and low) β to 5. Training for 30 epochs for a base-to-novel setting in the first 9 transformer layers. Training for 20 epochs for domain generalization setting and cross-dataset evaluation setting in the

Table 3. Domain generalization.

	Source	Target				
	ImageNet	-V2	-S	-A	-R	Average
CoOp	71.51	64.2	47.99	49.71	75.21	59.28
+ DePT	72.63	64.80	48.05	50.00	75.50	59.58
+ Ours	71.82	65.13	48.10	50.15	76.13	59.87
CoCoOp	71.02	64.07	48.75	50.63	76.18	59.91
+ DePT	72.77	65.10	49.10	51.00	76.85	60.51
+ Ours	72.10	65.25	50.13	52.11	77.18	61.16
MaPLe	70.72	64.07	49.15	50.9	76.98	60.27
+ DePT	73.27	65.33	49.05	51.25	77.50	60.78
+ Ours	71.56	65.45	50.33	52.32	78.10	61.55
PromptSRC	71.27	64.35	49.55	50.90	77.80	60.65
+ DePT	71.60	64.51	50.15	51.88	77.18	60.93
+ Ours	71.41	65.50	51.33	52.00	78.85	61.92
FAP	72.00	64.40	49.55	51.00	77.00	60.48

first 3 transformer layers. We use an SGD optimizer with a learning rate of 0.0025 on a single GPU. Following the hand-crafted CLIP, we use the hand-crafted template sets from (Radford et al., 2021).

4.2. Datasets

In Table 5, the datasets cover multiple recognition tasks. These datasets are all open-source datasets. We conducted base-to-novel generalization experiments, few-shot learning experiments, and cross-dataset generalization experiments on 11 datasets. We conduct domain generalization experiments on four variant datasets.

4.3. Base-to-Novel Generalization Task

In the base-to-novel generalization task, the datasets are divided into base and novel classes. The model is trained on the base classes in a 16-shot setting, and tested on both the base and novel classes across 11 different datasets. The number of classes for base and novel is the same, which means that all classes in a dataset are evenly divided into two groups of classes. The process of dividing all classes in the dataset is randomly selected. HM refers to harmonic mean. This experiment evaluates the generalization ability of methods. In Table 2, our method demonstrates significant improvements on all 11 datasets on HM. Our method significantly enhances the performance of base classes while also improving the accuracy of zero-shot CLIP on novel classes. In terms of average performance, our method based on PromptSRC (s) attains 85.70% accuracy on the base classes, and 77.35% accuracy on the novel classes. Our method, as an easy-to-use module, achieves performance improvements for various baseline frameworks, such as CoOp, CoCoOp, MaPLe (M), and PromptSRC (S).

4.4. Cross-Dataset Generalization Task

We train our model with 16 shots on ImageNet and test on 10 other unseen datasets. This experiment aims to validate the potential of our method in a wide range of cross-dataset transfers. Our method for training ImageNet is lower than that of DePT. As shown in Table 4, our method based on PromptSRC shows competitive performance in 10/10 over the generic and flexible method DePT. These findings suggest that our method excels in achieving better generalization across a diverse range of unseen datasets.

4.5. Domain Generalization Task

We train our model using the ImageNet in 16 shots and test its performance on 4 different variants of the ImageNet. In Table 3, our method based on PromptSRC demonstrates the highest average improvement of 1.27% over the PromptSRC method. Additionally, when compared to DePT, our method consistently outperforms it across all ImageNet variant datasets. This indicates that our method is designed to enhance domain generalization.

5. Further Studies

5.1. Learning Depth and Embeddings Length

In Table 6, we note that increasing the learning depth generally increases the performance based on PromptSRC. As the number of layers increases to 11, the HM value decreases. It indicates excessive fine-tuning of the model, causing it to lose CLIP generalization. In Table 7, our findings indicate that the performance based on PromptSRC reaches its peak when the length of embeddings is set to 4 on HM for an average of 11 datasets. Our ablation studies are based on keeping all other settings unchanged.

5.2. Analysis of γ for \mathcal{L}_{CL}

In Table 8, it is observed that as the number of γ to 0.1, there is a peak in HM for an average of 11 datasets. We conduct analysis based on the PromptSRC model.

5.3. Analysis of Top- β and Low- β

In Table 9, it is observed that as the number of Top- β and Low- β to 5, there is a peak in HM (81.32%). We conduct analysis based on the PromptSRC model for an average of 11 datasets. We keep other hyperparameters unchanged.

5.4. Applying to Other ViT Instances

In Table 10, we apply our method in various types of ViT instances. Our experimental performance is based on the average performance of 11 datasets. Our generic and flexible module based on PromptSRC has the lowest performance of

Table 4. Cross-dataset generalization. Our method achieves overall favorable performance.

	Source				Target							
	ImageNet	Caltech101	OxfordPets	StanfordCars	Flowers102	Food101	Aircraft	SUN397	DTD	EuroSAT	UCF101	Average
CoOp (Zhou et al., 2022b)	71.51	93.70	89.14	64.51	68.71	85.30	18.47	64.15	41.92	46.39	66.55	63.88
+ DePT	72.63	93.30	90.00	65.53	70.50	85.97	21.90	66.07	43.17	44.97	68.80	65.02
+ Ours	71.82	94.10	90.33	65.82	70.01	86.10	20.71	65.11	43.98	46.55	68.00	65.07
CoCoOp (Zhou et al., 2022a)	71.02	94.43	90.14	65.32	71.88	86.06	22.94	67.36	45.73	45.37	68.21	65.74
+ DePT	72.77	94.10	90.63	66.23	72.17	86.27	22.90	67.30	45.50	44.17	69.53	65.88
+ Ours	72.10	94.88	90.57	65.80	72.15	87.00	22.78	68.12	45.98	46.15	69.10	66.25
MaPLe (Khattak et al., 2023a)	70.72	93.53	90.49	65.57	72.23	86.20	24.74	67.01	46.49	48.06	68.69	66.30
+ DePT	73.27	92.53	90.10	64.60	70.10	85.57	23.63	66.40	45.03	40.13	67.53	64.56
+ Ours	71.56	94.00	90.91	65.92	73.10	86.78	24.33	68.35	46.13	49.01	68.81	66.73
PromptSRC (Khattak et al., 2023b)	71.27	93.60	90.25	65.70	70.25	86.15	23.90	67.10	46.87	45.50	68.75	65.81
+ DePT	71.60	93.80	90.13	66.00	70.93	86.27	24.30	67.23	46.60	45.83	69.10	66.02
+ Ours	71.41	94.95	92.14	66.50	73.25	87.53	25.81	68.10	49.01	49.20	69.74	67.62
FAP (Zhou et al., 2024)	72.00	93.40	90.15	65.61	70.13	85.89	23.70	67.88	45.98	45.12	68.99	65.68

ViT-B/32, with a value of 79.70%. And, our method, which leverages PromptSRC, achieves the best performance with ViT-L/14, with a value of 84.20%.

5.5. Inference Stage Computational Cost

In Table 11, the compute cost analysis is performed using the SUN397 dataset over 10 epochs on a single GPU. While our method (row 3) may have a slower inference speed as a result of multiple cosine similarity calculations. The number of parameters we introduced has remained relatively consistent and stable in training. This implies that usually, our parameter quantity is lower than that of DePT.

6. Related Work

6.1. Vision Language Models

Recently, researchers have demonstrated the strong generalization capability of Visual Language Models (VLMs) (Alayrac et al., 2022) which involve training on large-scale datasets of image-text pairs. Such as CLIP (Radford et al., 2021), which is a prominent and straightforward framework among existing VLMs. The strong generalization capability of CLIP has made it a foundation for many methods in adapting pre-trained VLMs for downstream tasks (Sanghi et al., 2022; Maaz et al., 2022; Bangalath et al., 2022; Zhang et al., 2021). To enhance the generalization ability of VLMs, researchers have explored various approaches. Some approaches involve enhancing the text encoder or the visual encoder (Vaswani et al., 2017). By improving the capabilities of the text encoder, the model

can better capture the semantics and contextual information in the textual input. Similarly, enhancing the visual encoder allows the model to extract more informative and discriminative features from the visual input. Another approaches deeply fuse the visual and text knowledge within the model. Using a large number of images for training is indeed one of the most effective methods.

6.2. Prompt Tuning in Vision Language Models

Prompt tuning (Lester et al., 2021) is a commonly employed technique in the field of Natural Language Processing (NLP) for training on downstream tasks. Leveraging text prompts, which are instructions given to the language model component of VLMs, is a prevalent practice to improve task comprehension. Full fine-tuning and linear probes are two commonly employed approaches for adapting VLMs to downstream tasks. However, the constraints of both methods have prompted research into innovative techniques influenced by prompt tuning within the realm of Natural Language Processing. CoOp (Zhou et al., 2022b) and CoCoOp (Zhou et al., 2022a) fine-tuning the CLIP model for few-shot image recognition by optimizing a continuous set of embeddings within the textual branch. The image-conditional prompt utilized in CoCoOp significantly contributes to improving generalization to unseen classes. Moreover, some approaches (Yao et al., 2023b;a) constrain the proposed learnable prompts contain the essential general knowledge and prior distribution learning. By conditioning prompts on visual features, CoCoOp (Zhou et al., 2022a) ensures that the language model focuses on pertinent visual information when making predictions. In addition to prompt tuning, ap-

Table 5. Training and testing datasets. dataset consists of 11 image classification datasets and four variant datasets of ImageNet.

Dataset	Classes	Train	Val	Test
ImageNet (Deng et al., 2009)	1,000	1.28 M	N/A	50,000
Caltech101 (Fei-Fei et al., 2004)	100	4,128	1,649	2,465
OxfordPets (Parkhi et al., 2012)	37	2,944	736	3,669
StanfordCars (Krause et al., 2013)	196	6,509	1,635	8,041
Flowers102 (Nilsback & Zisserman, 2008)	102	4,093	1,633	2,463
Food101 (Bossard et al., 2014)	101	50,500	20,200	30,300
FGVCAircraft (Maji et al., 2013)	100	3,334	3,333	3,333
SUN397 (Xiao et al., 2010)	397	15,880	3,970	19,850
DTD (Cimpoi et al., 2014)	47	2,820	1,128	1,692
EuroSAT (Helber et al., 2019)	10	13,500	5,400	8,100
UCF101 (Soomro et al., 2012)	101	7,639	1,898	3,783
-V2 (Recht et al., 2019)	1,000	N/A	N/A	10,000
-Sketch (Wang et al., 2019)	1,000	N/A	N/A	50,889
-A (Hendrycks et al., 2021b)	200	N/A	N/A	7,500
-R (Hendrycks et al., 2021a)	200	N/A	N/A	30,000

Table 6. Analysis of learning depth based on PromptSRC for an average of 11 datasets.

Learning Depth	1	3	5	7	9	11
HM	77.11	78.03	79.12	80.01	81.32	80.21

Table 7. Analysis of embeddings length based on PromptSRC for an average of 11 datasets.

Prompt Length	1	2	4	6	8	10
HM	77.01	80.05	81.32	80.30	79.11	78.54

 Table 8. Analysis of γ for \mathcal{L}_{CL} in pre-trained features matrix. We conduct analysis based on the PromptSRC (Khattak et al., 2023b) model for an average of 11 datasets. HM refers to harmonic mean.

Average (11 datasets)				
	0.05	0.1	0.5	0.9
HM (γ)	80.13	81.32	81.00	79.88

 Table 9. Identifying scores of Top- β and Low- β for an average of 11 datasets. We conduct analysis based on the PromptSRC (Khattak et al., 2023b) model. HM refers to harmonic mean.

Average (11 datasets)				
	3	4	5	6
HM (β)	78.21	79.81	81.32	80.51

proach (Zhang et al., 2024) introduces a generic and flexible approach to align its vision and language representations.

Table 10. Applying to other ViT instances.

Average (11 datasets)			
	ViT-B/32	ViT-B/16	ViT-L/14
HM (ViT)	79.70	81.32	84.20

Table 11. The compute cost analysis is performed using the SUN397 (Xiao et al., 2010) dataset over 10 epochs on a single GPU. ‘N’: the num of classes in the base task (Zhang et al., 2024).

Method	Train time	Learnable para.	HM
CoOp	10.88min	8K	71.65
+ DePT	10.91min	+ (2+N/2)K	77.30
+ Ours	13.56min	+ 3072	78.66

7. Limitations and Conclusion

Due to our method incorporating multiple contrastive learning processes, the training speed is slower. Moreover, we plan to investigate the potential of our method in other downstream tasks (Sanghi et al., 2022).

In this paper, we propose a Features Matrix (FM) for vision-language models. Our method incorporates multiple hand-crafted prompts to extract general information as a pre-trained features matrix from CLIP to enhance generalization. The matrix of pre-trained features can delve into the semantics of different hand-crafted prompts at a more profound level, which reduces the risk of forgetting the essential general knowledge of pre-trained CLIP. Importantly, our method is compatible with representative prompt learning frameworks for textual or multi-modal prompts as a generic and flexible module.

Impact Statement

This paper presents work whose goal is to advance the field of Machine Learning. None of these points we feel must be specifically highlighted here.

References

- Alayrac, J.-B., Donahue, J., Luc, P., Miech, A., Barr, I., Hasson, Y., Lenc, K., Mensch, A., Millican, K., Reynolds, M., et al. Flamingo: a visual language model for few-shot learning. *Advances in Neural Information Processing Systems*, 35:23716–23736, 2022.
- Bangalath, H., Maaz, M., Khattak, M. U., Khan, S. H., and Shahbaz Khan, F. Bridging the gap between object and image-level representations for open-vocabulary detection. *Advances in Neural Information Processing Systems*, 35:33781–33794, 2022.
- Bossard, L., Guillaumin, M., and Van Gool, L. Food-101—mining discriminative components with random forests. In *Computer Vision—ECCV 2014: 13th European Conference, Zurich, Switzerland, September 6–12, 2014, Proceedings, Part VI 13*, pp. 446–461. Springer, 2014.
- Chen, G., Yao, W., Song, X., Li, X., Rao, Y., and Zhang, K. Plot: Prompt learning with optimal transport for vision-language models. *arXiv preprint arXiv:2210.01253*, 2022.
- Chen, T., Kornblith, S., Norouzi, M., and Hinton, G. A simple framework for contrastive learning of visual representations. In *International conference on machine learning*, pp. 1597–1607. PMLR, 2020.
- Cimpoi, M., Maji, S., Kokkinos, I., Mohamed, S., and Vedaldi, A. Describing textures in the wild. In *Proceedings of the IEEE conference on computer vision and pattern recognition*, pp. 3606–3613, 2014.
- Deng, J., Dong, W., Socher, R., Li, L.-J., Li, K., and Fei-Fei, L. Imagenet: A large-scale hierarchical image database. In *2009 IEEE conference on computer vision and pattern recognition*, pp. 248–255. Ieee, 2009.
- Dosovitskiy, A., Beyer, L., Kolesnikov, A., Weissenborn, D., Zhai, X., Unterthiner, T., Dehghani, M., Minderer, M., Heigold, G., Gelly, S., et al. An image is worth 16x16 words: Transformers for image recognition at scale. *arXiv preprint arXiv:2010.11929*, 2020.
- Etchegaray, D., Huang, Z., Harada, T., and Luo, Y. Find n’propagate: Open-vocabulary 3d object detection in urban environments. *arXiv preprint arXiv:2403.13556*, 2024.
- Fei-Fei, L., Fergus, R., and Perona, P. Learning generative visual models from few training examples: An incremental bayesian approach tested on 101 object categories. In *2004 conference on computer vision and pattern recognition workshop*, pp. 178–178. IEEE, 2004.
- Greer, R., Antoniussen, B., Andersen, M. V., Møgelmoose, A., and Trivedi, M. M. The why, when, and how to use active learning in large-data-driven 3d object detection for safe autonomous driving: An empirical exploration. *arXiv preprint arXiv:2401.16634*, 2024.
- Helber, P., Bischke, B., Dengel, A., and Borth, D. Eurosat: A novel dataset and deep learning benchmark for land use and land cover classification. *IEEE Journal of Selected Topics in Applied Earth Observations and Remote Sensing*, 12(7):2217–2226, 2019.
- Hendrycks, D., Basart, S., Mu, N., Kadavath, S., Wang, F., Dorundo, E., Desai, R., Zhu, T., Parajuli, S., Guo, M., et al. The many faces of robustness: A critical analysis of out-of-distribution generalization. In *Proceedings of the IEEE/CVF International Conference on Computer Vision*, pp. 8340–8349, 2021a.
- Hendrycks, D., Zhao, K., Basart, S., Steinhardt, J., and Song, D. Natural adversarial examples. In *Proceedings of the IEEE/CVF Conference on Computer Vision and Pattern Recognition*, pp. 15262–15271, 2021b.
- Jia, M., Tang, L., Chen, B.-C., Cardie, C., Belongie, S., Hariharan, B., and Lim, S.-N. Visual prompt tuning. In *European Conference on Computer Vision*, pp. 709–727. Springer, 2022.
- Khattak, M. U., Rasheed, H., Maaz, M., Khan, S., and Khan, F. S. Maple: Multi-modal prompt learning. In *Proceedings of the IEEE/CVF Conference on Computer Vision and Pattern Recognition*, pp. 19113–19122, 2023a.
- Khattak, M. U., Wasim, S. T., Naseer, M., Khan, S., Yang, M.-H., and Khan, F. S. Self-regulating prompts: Foundational model adaptation without forgetting. In *Proceedings of the IEEE/CVF International Conference on Computer Vision*, pp. 15190–15200, 2023b.
- Krause, J., Stark, M., Deng, J., and Fei-Fei, L. 3d object representations for fine-grained categorization. In *Proceedings of the IEEE international conference on computer vision workshops*, pp. 554–561, 2013.
- Langley, P. Crafting papers on machine learning. In Langley, P. (ed.), *Proceedings of the 17th International Conference on Machine Learning (ICML 2000)*, pp. 1207–1216, Stanford, CA, 2000. Morgan Kaufmann.
- Lester, B., Al-Rfou, R., and Constant, N. The power of scale for parameter-efficient prompt tuning. *arXiv preprint arXiv:2104.08691*, 2021.

- Lu, Y., Liu, J., Zhang, Y., Liu, Y., and Tian, X. Prompt distribution learning. In *Proceedings of the IEEE/CVF Conference on Computer Vision and Pattern Recognition*, pp. 5206–5215, 2022.
- Maaz, M., Rasheed, H., Khan, S., Khan, F. S., Anwer, R. M., and Yang, M.-H. Class-agnostic object detection with multi-modal transformer. In *European Conference on Computer Vision*, pp. 512–531. Springer, 2022.
- Maji, S., Rahtu, E., Kannala, J., Blaschko, M., and Vedaldi, A. Fine-grained visual classification of aircraft. *arXiv preprint arXiv:1306.5151*, 2013.
- Nilsback, M.-E. and Zisserman, A. Automated flower classification over a large number of classes. In *2008 Sixth Indian conference on computer vision, graphics & image processing*, pp. 722–729. IEEE, 2008.
- Parkhi, O. M., Vedaldi, A., Zisserman, A., and Jawahar, C. Cats and dogs. In *2012 IEEE conference on computer vision and pattern recognition*, pp. 3498–3505. IEEE, 2012.
- Radford, A., Kim, J. W., Hallacy, C., Ramesh, A., Goh, G., Agarwal, S., Sastry, G., Askell, A., Mishkin, P., Clark, J., et al. Learning transferable visual models from natural language supervision. In *International conference on machine learning*, pp. 8748–8763. PMLR, 2021.
- Recht, B., Roelofs, R., Schmidt, L., and Shankar, V. Do imagenet classifiers generalize to imagenet? In *International conference on machine learning*, pp. 5389–5400. PMLR, 2019.
- Sanghi, A., Chu, H., Lambourne, J. G., Wang, Y., Cheng, C.-Y., and Fumero, M. Clip-forge: Towards zero-shot text-to-shape generation. *arXiv preprint arXiv:2110.02624*, 2021.
- Sanghi, A., Chu, H., Lambourne, J. G., Wang, Y., Cheng, C.-Y., Fumero, M., and Malekshan, K. R. Clip-forge: Towards zero-shot text-to-shape generation. In *Proceedings of the IEEE/CVF Conference on Computer Vision and Pattern Recognition*, pp. 18603–18613, 2022.
- Soomro, K., Zamir, A. R., and Shah, M. Ucf101: A dataset of 101 human actions classes from videos in the wild. *arXiv preprint arXiv:1212.0402*, 2012.
- Vaswani, A., Shazeer, N., Parmar, N., Uszkoreit, J., Jones, L., Gomez, A. N., Kaiser, Ł., and Polosukhin, I. Attention is all you need. *Advances in neural information processing systems*, 30, 2017.
- Wang, H., Ge, S., Lipton, Z., and Xing, E. P. Learning robust global representations by penalizing local predictive power. *Advances in Neural Information Processing Systems*, 32, 2019.
- Xiao, J., Hays, J., Ehinger, K. A., Oliva, A., and Torralba, A. Sun database: Large-scale scene recognition from abbey to zoo. In *2010 IEEE computer society conference on computer vision and pattern recognition*, pp. 3485–3492. IEEE, 2010.
- Yao, H., Zhang, R., and Xu, C. Visual-language prompt tuning with knowledge-guided context optimization. In *Proceedings of the IEEE/CVF Conference on Computer Vision and Pattern Recognition (CVPR)*, pp. 6757–6767, June 2023a.
- Yao, H., Zhang, R., and Xu, C. Visual-language prompt tuning with knowledge-guided context optimization. In *Proceedings of the IEEE/CVF Conference on Computer Vision and Pattern Recognition*, pp. 6757–6767, 2023b.
- Zhang, J., Wu, S., Gao, L., Shen, H. T., and Song, J. Dept: Decoupled prompt tuning. In *Proceedings of the IEEE/CVF Conference on Computer Vision and Pattern Recognition*, pp. 12924–12933, 2024.
- Zhang, R., Fang, R., Zhang, W., Gao, P., Li, K., Dai, J., Qiao, Y., and Li, H. Tip-adapter: Training-free clip-adapter for better vision-language modeling. *arXiv preprint arXiv:2111.03930*, 2021.
- Zhou, K., Yang, J., Loy, C. C., and Liu, Z. Conditional prompt learning for vision-language models. In *Proceedings of the IEEE/CVF Conference on Computer Vision and Pattern Recognition*, pp. 16816–16825, 2022a.
- Zhou, K., Yang, J., Loy, C. C., and Liu, Z. Learning to prompt for vision-language models. *International Journal of Computer Vision*, 130(9):2337–2348, 2022b.
- Zhou, Y., Xia, X., Lin, Z., Han, B., and Liu, T. Few-shot adversarial prompt learning on vision-language models. *Advances in Neural Information Processing Systems*, 37: 3122–3156, 2024.

A. Appendix for “Enhancing Target-unspecific Tasks through a Features Matrix”.

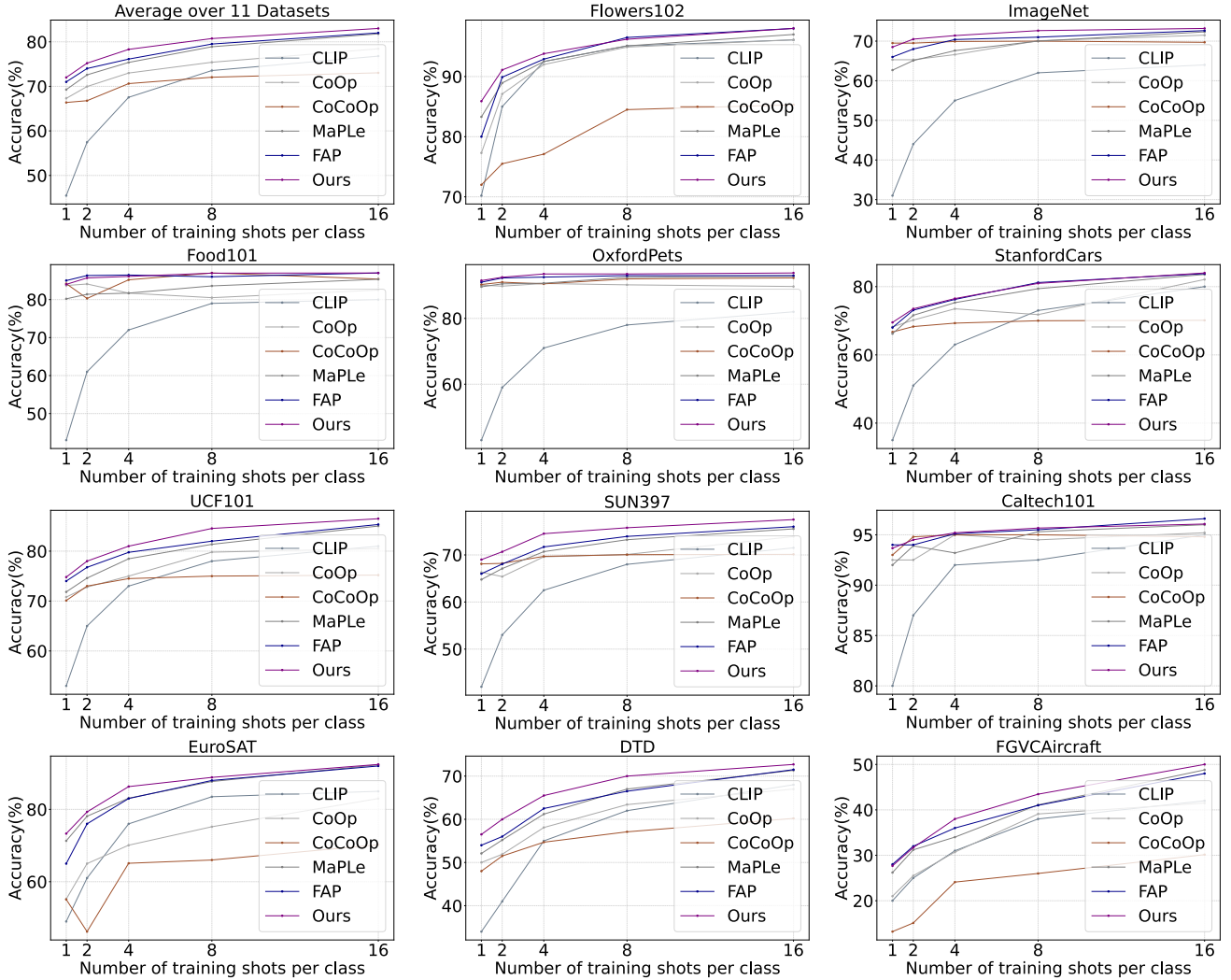


Figure 4. Additional non-generalized task for auxiliary experiments. Our method based on PromptSRC maintains enhanced performance.

A.1. Additional Non-Generalized Task

In this paper, the primary aim of our method is to tackle generalization tasks. Additionally, we explore whether our method can also be performed in non-generalized tasks for auxiliary experiments.

We train and test the model on 11 datasets by conducting with varying K -shots per class, where K takes the values of 1, 2, 4, 8, and 16. We analyze the effectiveness of target-specific tasks based on PromptSRC with limited labeled data. Our method (purple line) achieves larger gains in minimal cases such as for $K = 4$ for almost datasets. This highlights the effect of our designs in enhancing target-specific recognition with limited labeled data. Compared with the existing state-of-the-art few-shot FAP (NIPS2024) (Zhou et al., 2024), our method performs in no-generalization classification effectively for an average of over 11 datasets, as shown in Figure 4 (left-top).

A.2. Base-to-Novel Generalization Task

In Table 16, we conducted base-to-novel generalization experiments in the appendix and compared them in **detail** with an easy-to-use DePT (Zhang et al., 2024) (CVPR2024) and FAP (Zhou et al., 2024) (NIPS2024). We found that our performance is higher than DePT when integrated with different methods.

A.3. Hand-Crafted Prompt Templates

The hand-crafted prompt template used in this paper is as follows (Radford et al., 2021):

"a photo of a .",
 "a bad photo of a .", "a photo of many .",
 "a sculpture of a .", "a photo of the hard to see .",
 "a low resolution photo of the .", "a rendering of a .",
 "graffiti of a .", "a bad photo of the .",
 "a cropped photo of the .", "a tattoo of a .",
 "the embroidered .", "a photo of a hard to see .",
 "a bright photo of a .", "a photo of a clean .",
 "a photo of a dirty .", "a dark photo of the .",
 "a drawing of a .", "a photo of my .",
 "the plastic .", "a photo of the cool .",
 "a close-up photo of a .", "a black and white photo of the .",
 "a painting of the .", "a painting of a .",
 "a pixelated photo of the .", "a sculpture of the .",
 "a bright photo of the .", "a cropped photo of a .",
 "a plastic .", "a photo of the dirty .",
 "a jpeg corrupted photo of a .", "a blurry photo of the .",
 "a photo of the .", "a good photo of the .",
 "a rendering of the .", "a in a video game.",
 "a photo of one .", "a doodle of a .",
 "a close-up photo of the .", "the origami .",
 "the in a video game.", "a sketch of a .",
 "a doodle of the .", "a origami .",
 "a low resolution photo of a .", "the toy .",
 "a rendition of the .", "a photo of the clean .",
 "a photo of a large .", "a rendition of a .",
 "a photo of a nice .",
 "a photo of a weird .",
 "a blurry photo of a .",
 "a cartoon .",

”art of a .”,
 ”a sketch of the .”,
 ”a embroidered .”,
 ”a pixelated photo of a .”,
 ”itap of the .”,

A.4. Learning Depth and Embeddings Length

In Table 12, as the number of layers increases to 11, the HM value decreases. It indicates excessive fine-tuning of the model, causing it to lose CLIP generalization. In Table 13, our findings indicate that the performance based on PromptSRC reaches its peak when the length of embeddings is set to 4 on base-to-novel generalization (HM) for Caltech101 (Fei-Fei et al., 2004) and Food101 (Bossard et al., 2014).

Table 12. Analysis of learning depth based on PromptSRC.

Prompt Depth	1	3	5	7	9	11
HM (Caltech101)	90.99	92.43	95.76	96.81	97.27	95.87
HM (Food101)	86.11	87.90	88.21	90.00	91.45	90.53

Table 13. Analysis of embeddings length based on PromptSRC.

Prompt Length	1	2	4	6	8	10
HM (Caltech101)	95.55	96.21	97.27	96.30	95.88	94.11
HM (Food101)	89.00	90.11	91.45	89.34	88.01	87.54

A.5. Analysis of γ for \mathcal{L}_{CL}

In Table 14, it is observed that as the number of γ to 0.1, there is a peak in HM for Caltech101 and Food101.

Table 14. Analysis of γ for \mathcal{L}_{CL} in pre-trained features matrix. We conduct analysis based on the PromptSRC (Khattak et al., 2023b) model. HM refers to harmonic mean.

	Caltech101				Food101			
	0.05	0.1	0.5	0.9	0.05	0.1	0.5	0.9
HM (γ)	97.01	97.27	96.65	95.11	90.33	91.45	90.53	89.50

A.6. Analysis of Top- β and Low- β

In Table 15, it is observed that as the number of Top- β and Low- β to 5, there is a peak in HM (Chen et al., 2020).

Table 15. Identifying scores of Top- β and Low- β for Caltech101 and Food101. We conduct analysis based on the PromptSRC (Khattak et al., 2023b) model. HM refers to harmonic mean.

	Caltech101				Food101			
	3	4	5	6	3	4	5	6
HM (β)	95.71	96.80	97.27	96.11	88.12	89.90	91.45	90.13

Table 16. Base-to-novel generalization. Compared with FAP (NIPS2024) and an easy-to-use DePT (CVPR2024) in detail, our method achieves consistent average performance improvement over different representative baselines (CoOp, CoCoOp, MaPLe, PromptSRC).

(a) Average over 11 datasets				(b) ImageNet				(c) Caltech101				(d) OxfordPets			
Base	Novel	HM		Base	Novel	HM		Base	Novel	HM		Base	Novel	HM	
CoOp	82.69	63.22	71.66	CoOp	76.47	67.88	71.92	CoOp	98.00	89.81	93.73	CoOp	93.67	95.29	94.47
+DePT	83.66	71.82	77.29	+DePT	77.13	70.10	73.45	+DePT	98.33	94.33	96.29	+DePT	94.70	97.63	96.14
+ Ours	81.15	74.66	77.79	+ Ours	75.85	71.33	73.53	+ Ours	97.58	96.60	97.13	+ Ours	93.78	97.80	95.78
Co	80.47	71.69	75.83	Co	75.98	70.43	73.10	Co	97.96	93.81	95.84	Co	95.20	97.69	96.43
+DePT	83.80	72.89	77.97	+DePT	76.87	70.47	73.53	+DePT	98.37	93.87	96.06	+DePT	94.03	97.20	95.59
+ Ours	81.68	75.55	78.52	+ Ours	77.35	72.36	74.79	+ Ours	98.61	96.75	97.70	+ Ours	95.33	98.15	96.76
M	82.28	75.14	78.55	M	76.66	70.54	73.47	M	97.74	94.36	96.02	M	95.43	97.76	96.58
+DePT	84.85	74.82	79.52	+DePT	77.87	70.23	73.85	+DePT	98.53	95.03	96.75	+DePT	95.03	97.83	96.41
+ Ours	84.45	76.53	80.32	+ Ours	78.18	71.38	74.62	+ Ours	98.35	96.11	97.22	+ Ours	95.85	98.22	97.04
S	84.26	76.10	79.97	S	77.60	70.73	74.01	S	98.10	94.03	96.02	S	95.33	97.30	96.30
+ DePT	85.19	76.17	80.43	+ DePT	78.20	70.27	74.02	+ DePT	98.57	94.10	96.28	+ DePT	95.43	97.33	96.37
+ Ours	85.70	77.35	81.32	+ Ours	78.90	71.58	75.07	+ Ours	98.62	95.88	97.27	+ Ours	95.95	97.92	96.95
FAP	84.22	76.95	80.45	FAP	77.00	71.40	74.10	FAP	97.85	95.05	96.43	FAP	95.00	97.30	96.19
(e) EuroSAT				(f) UCF101				(g) StanfordCars				(h) Flowers102			
Base	Novel	HM		Base	Novel	HM		Base	Novel	HM		Base	Novel	HM	
CoOp	92.19	54.74	68.69	CoOp	84.69	56.05	67.46	CoOp	78.12	60.40	68.13	CoOp	97.60	59.67	74.06
+DePT	88.27	66.27	75.70	+ DePT	85.43	72.17	78.24	+ DePT	79.67	72.40	75.86	+ DePT	98.20	72.00	83.08
+ Ours	88.35	65.33	75.13	+ Ours	83.10	78.85	80.94	+ Ours	74.32	76.87	75.58	+ Ours	96.22	72.32	82.57
Co	87.49	60.04	71.21	Co	82.33	73.45	77.64	Co	70.49	73.59	72.01	Co	94.87	71.75	81.71
+DePT	90.27	66.87	76.82	+ DePT	85.70	72.80	78.73	+ DePT	79.87	73.33	76.46	+ DePT	98.33	72.57	83.51
+ Ours	88.15	70.11	78.12	+ Ours	82.95	77.21	80.00	+ Ours	72.88	76.10	74.46	+ Ours	95.61	74.93	84.03
M	94.07	73.23	82.35	M	83.00	78.66	80.77	M	72.94	74.00	73.47	M	95.92	72.46	82.56
+DePT	94.43	76.23	84.36	+ DePT	86.87	78.10	82.25	+ DePT	80.93	71.73	76.06	+ DePT	98.03	73.17	83.79
+ Ours	94.22	75.65	83.93	+ Ours	87.33	79.10	83.02	+ Ours	78.66	75.13	76.86	+ Ours	98.21	75.00	85.07
S	92.90	73.90	82.32	S	87.10	78.80	82.74	S	78.27	74.97	76.58	S	98.07	76.50	85.95
+ DePT	92.23	77.90	84.88	+ DePT	87.73	77.70	82.46	+ DePT	80.80	75.00	77.79	+ DePT	98.40	77.10	86.46
+ Ours	95.50	76.85	85.17	+ Ours	88.80	79.50	83.93	+ Ours	80.91	76.51	78.68	+ Ours	98.81	78.10	87.26
FAP	94.55	75.89	83.40	FAP	86.30	79.98	82.70	FAP	81.33	74.85	77.88	FAP	96.85	77.86	85.54
(i) Food101				(j) FGVC Aircraft				(k) SUN397				(l) DTD			
Base	Novel	HM		Base	Novel	HM		Base	Novel	HM		Base	Novel	HM	
CoOp	88.33	82.26	85.19	CoOp	40.44	22.30	28.75	CoOp	80.60	65.89	72.51	CoOp	79.44	41.18	54.24
+ DePT	90.43	91.33	90.88	+ DePT	42.53	22.53	29.46	+ DePT	82.37	75.07	78.55	+ DePT	83.20	56.13	67.04
+ Ours	89.98	92.85	91.41	+ Ours	37.32	34.61	35.92	+ Ours	79.12	78.38	78.77	+ Ours	77.10	56.38	65.15
Co	90.70	91.29	90.99	Co	33.41	23.71	27.74	Co	79.74	76.86	78.27	Co	77.01	56.00	64.85
+ DePT	90.30	91.30	90.80	+ DePT	43.07	31.30	36.25	+ DePT	82.20	76.73	79.37	+ DePT	82.77	55.40	66.37
+ Ours	90.61	91.93	91.28	+ Ours	37.87	34.91	36.33	+ Ours	80.32	79.00	79.68	+ Ours	78.90	59.61	67.93
M	90.71	92.05	91.38	M	37.44	35.61	36.50	M	80.82	78.70	79.75	M	80.36	59.18	68.16
+ DePT	90.33	91.53	90.93	+ DePT	44.53	32.80	37.78	+ DePT	82.90	76.40	79.52	+ DePT	83.87	59.93	69.91
+ Ours	90.31	92.81	91.57	+ Ours	42.46	37.62	39.89	+ Ours	82.35	79.81	81.07	+ Ours	83.01	60.98	70.32
S	90.67	91.53	91.10	S	42.73	37.87	40.15	S	82.67	78.47	80.52	S	83.37	62.97	71.75
+ DePT	90.87	91.57	91.22	+ DePT	45.70	36.73	40.73	+ DePT	83.27	78.97	81.06	+ DePT	84.80	61.20	71.09
+ Ours	90.61	92.30	91.45	+ Ours	45.81	39.11	42.20	+ Ours	83.90	80.51	82.20	+ Ours	84.90	62.58	72.07
FAP	91.05	92.56	91.82	FAP	41.56	39.75	40.03	FAP	82.85	78.77	80.62	FAP	82.10	63.11	70.42